Image Fusion of Spectrally Nonoverlapping Imagery Using SPCA and MTF-Based Filters

Yonghyun Kim, Minho Kim, Jaewan Choi, and Yongil Kim

***Abstract*— Most spaceborne sensors have an inevitable tradeoff between spatial and spectral resolutions. This is a typical ill-posed inverse problem in the field of image fusion. To solve this problem, this letter proposes an image fusion method using spatial principal component analysis and modulation transfer function-based filters. The key behind the proposed fusion method is to efficiently estimate the missing spatial details by considering the spatial structures of the low-resolution multispectral (MS) imagery. Also, this letter proposes a newly developed injection gain model to resolve the local and global dissimilarity between panchromatic and MS imageries, which could prevent over- and under-injections. Finally, spatial details, optimized to be injected into the MS images, were constructed and paired with the developed injection gain model to produce high-resolution MS images. Two data sets acquired by WorldView-2 are employed for validation. The experimental results demonstrate that the proposed fusion method generates high-quality imagery in terms of both qualitative and quantitative standards.**

***Index Terms*— Image fusion, injection gain, modulation transfer function (MTF), spatial principal component analysis (SPCA), WorldView-2.**

I. Introduction

THE tradeoff between spatial and spectral resolutions of satellite sensors is a lingering design constraint in the field of remote sensing [1]. To overcome this design constraint effectively, image fusion or pansharpening methods have been used [2]. The fusion of panchromatic (PAN) and multispectral (MS) imageries, in addition to hyperspectral (HS) images [3], has thus become a key preprocessing step in many geospatial applications.

In the last few decades, various image fusion methods have been suggested to address the issues regarding the fusion of remotely sensed imagery. Generally, image fusion methods can be classified into two approaches: the *component substitution* (CS) methods and the *multiresolution analysis* (MRA) techniques [2], [3]. While the two approaches possess their respective strengths and weaknesses, there are also hybrid fusion methods which integrate the two methods. More recently, the sparse representation (SR)-based fusion method [4] and fusion methods that apply edge-preserving filters, such as guided filter [5] and bilateral filters [6], have been proposed and are well suited for image fusion.

In general, visible bands of MS images are included in the spectral range of the broadband PAN image [7]. As a result, most image fusion methods assume a partial positive correlation between PAN and MS images. For spectrally nonoverlapping MS bands with respect to the PAN band, however, the difference of spectral ranges disproves this assumption of linearity or correlation with each other. In particular, recently launched satellite sensors, such as WorldView-2 and -3, have certain spectrally nonoverlapping MS bands with respect to the PAN band. An effective image fusion method for these sensors is, therefore, required, which if generated to a high spatial resolution can detect numerous, undistinguishable features in visible bands and by human vision [8] and can thus be applied in various fields such as vegetation, disasters, and geology [9].

There are largely two issues with the image fusion of spectrally nonoverlapping bands that need to be addressed. First, developing a new injection gain model is required to resolve the local and global dissimilarity in radiometry between PAN and MS images [10]. Second, there is an issue with the effective extraction of spatial details injected into the MS images from the high-spatial-resolution PAN image. To address these issues, a new injection gain model is proposed, which infers the spatial details and transfers them to the MS bands. Also, the recently proposed spatial principal component analysis (PCA) [11] and modulation transfer function (MTF)-based filters [12], which consider the spatial structures of the MS bands for the extraction of appropriate spatial details, were adopted and proposed in this letter.

The rest of this letter is structured as follows. Section II introduces a new injection gain model. The proposed image fusion method is presented in Section III, and Section IV presents the experiments and discusses the results. Last, the conclusion is provided in Section V.

II. Injection Gain Model Based on Edge Modulation

Generally, the first significant parameter needed to be addressed in image fusion is the injection gains that decide the degree of spatial details. However, spectrally mismatched MS and PAN bands share not only less radiometric information, but also geometric information, which makes inferring injection gains difficult. To address this issue, a new injection gain model derived by the edges of the MS, PAN, and low-resolution PAN images is proposed.

Manuscript received August 12, 2017; revised October 5, 2017; accepted October 9, 2017. Date of publication October 31, 2017; date of current version December 4, 2017. This work was supported by the National Research Foundation of Korea under Grant NRF-2015M1A3A3A02014673. *(Corresponding author: Yonghyun Kim.)*

Y. Kim, M. Kim, and Y. Kim are with the Department of Civil and Environmental Engineering, Seoul National University, Seoul 08826, South Korea (e-mail: yhkeen@gmail.com; kimminho93@gmail.com; yik@snu.ac.kr).

J. Choi is with the School of Civil Engineering, Chungbuk National University, Cheongju 28644, South Korea (e-mail: jaewanchoi@chungbuk.ac.kr).

Color versions of one or more of the figures in this letter are available online at http://ieeexplore.ieee.org.

Digital Object Identifier 10.1109/LGRS.2017.2762427

A. Edge-Induced Injection Gain

Rahmani *et al.* [13] proposed the following expression which uses $h(\mathbf{P})$ as an injection gain that controls the injection of spatial details:

$$h(\mathbf{P}) = \exp\left(-\frac{\lambda}{|\nabla \mathbf{P}| + \varepsilon}\right) \tag{1}$$

where $\nabla \mathbf{P}$ is the gradient of the PAN image, λ is a parameter indicating how large the gradient should be in order to be an edge and controlling the smoothness of the image, and ε is a small value that enforces a nonzero denominator. The parameter values that proved successful are $\lambda = 10^{-9}$ and $\varepsilon = 10^{-10}$, and the measurable range of $h(\mathbf{P})$ is limited from 0 to 1. However, this injection gain is unnatural because it only modulates the PAN-induced edges and is thus vulnerable to radiometric and geometric distortions, particularly in the spectrally mismatched MS bands with regard to the PAN band. To solve this limitation, another injection gain which simultaneously uses MS-induced edges was proposed in [14]; however, it is important to note that the manually selected tradeoff parameter between MS- and PAN-induced edges has a decisive effect on the fused imagery. As a result, selecting the wrong parameter could invoke not only radiometric, but also geometric distortions, especially for spectrally nonoverlapping MS and PAN bands.

B. Proposed Injection Gain Based on Edge Modulation

In this letter, in order to avoid radiometric distortion while maintaining the geometric details, we introduce a new injection gain which utilizes the low-resolution PAN image **LRP** in addition to available kth MS images $\widetilde{\mathbf{M}}_k$ and PAN image **P**-induced edges. To do this, we form the following new injection gain:

$$h\left(\widetilde{\mathbf{M}}_k, \mathbf{LRP}, \mathbf{P}\right) = \circ \frac{[h(\widetilde{\mathbf{M}}_k) + 1]}{[h(\mathbf{LRP}) + 1]} \circ [h(\mathbf{P}) + 2] \tag{2}$$

where $\circ$ denotes pixel-wise operations and $\widetilde{\mathbf{M}}_k$ represents upscaled MS images to the PAN size. **LRP** indicates a low-resolution PAN image using a Gaussian filter mimicking the MTF of the PAN band. In (2), we add 1 to each bracket of the denominator and numerator for numerical stability. As a result, adding a weight of 1 identically to $h(\widetilde{\mathbf{M}}_k)$ and $h(\mathbf{LRP})$ prevents extreme and nonnumerical values by avoiding the division of extremely small values or a zero denominator. The left part of (2) represents the relative edge-induced contribution at low-resolution scale resulting in a modulation of injected spatial details at high-resolution scale. In other words, for regions with high gradient energy in the ratio of $\widetilde{\mathbf{M}}_k$ and **LRP** images, their corresponding regions in the detail layer of the high-resolution scale will also contain high gradient energy. In addition, for $h(\mathbf{P})$, a value of 2 was added to double the weight of the spatial details of **P**. As a result, the range of $h(\widetilde{\mathbf{M}}_k, \mathbf{LRP}, \mathbf{P})$ was set to 1–6, but the range of the injection was relatively wide. To address this, values of (2) were normalized to a range of 0–1 and the correlation coefficients (Corr) of $\widetilde{\mathbf{M}}_k$ and **LRP** were added to avoid the unsharpening of $\widetilde{\mathbf{M}}_k$. In this case, Corr determines the similarity or linearity degree in terms of radiometric and geometric information at the low-resolution scale, which can then be used to determine the minimum degree of the injection. Finally, our proposed new injection gain $\mathbf{\Gamma}$ is obtained as

$$\mathbf{\Gamma} = [h(\widetilde{\mathbf{M}}_k, \mathbf{LRP}, \mathbf{P}) + \mathrm{Corr}(\widetilde{\mathbf{M}}_k, \ \mathbf{LRP})]. \tag{3}$$

In this letter, if the value of Corr is less than 0.5, the Corr value is set to 0.5. In summary, $h(\widetilde{\mathbf{M}}_k, \mathbf{LRP}, \mathbf{P})$ of (3) is a locally variant injection gain in a *context-adaptive* approach and $\mathrm{Corr}(\widetilde{\mathbf{M}}_k, \ \mathbf{LRP})$ of (3) is a global injection gain per spectral band. The proposed injection gain could, therefore, resolve the local and global dissimilarity between the PAN and MS images.

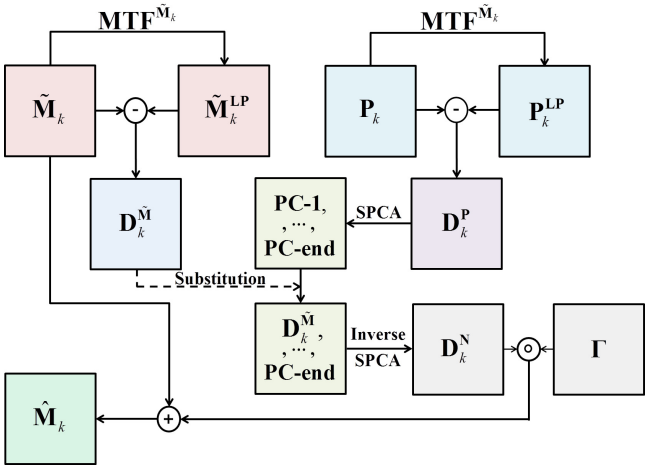

Fig. 1. Schematic of the proposed fusion method.

III. Proposed SPCA and MTF-Based Fusion Method

In [11], a new image fusion method utilizing the spatial PCA (SPCA) was proposed. The key advantage of the SPCA fusion method is that the interpolation of MS data is not needed, making the fusion method less prone to error from interpolating MS images to the same size as that of the PAN image. Nevertheless, given that the SPCA fusion method separates instead of overlapping each patch, blocking effects may occur in adjacent patches of the fused images. Certain features may, thus, be more accentuated than others because the features in one patch may appear more heterogeneous compared to those in another nearby patch. However, these windowing effects can be resolved by the overlapping approach. This letter, therefore, shows the use of the SPCA method as an overlapping method. In more detail, the fusion method proposed in this letter (see Fig. 1) exploits the SPCA method to construct the new spatial details which consider the local spatial structures of the MS images. To achieve this, the SPCA method was applied to the spatial details extracted from the PAN image, the first principal component (PC-1) was replaced with spatial details of the MS images, and inverse SPCA was applied to eliminate the unnecessary spatial redundancies of the PAN image, thereby rearranging the spatial details with reference to the spatial details of the MS images.

The key to pansharpening is to infer the spatial details from the known **P** and $\widetilde{\mathbf{M}}_k$. This is an extremely ill-posed

problem and thus, there are infinitely many solutions to construct the spatial details. Selecting an extraction model for suitable spatial details is a difficult task since it requires jointly characterizing the interrelation of $\mathbf{P}$ and $\widetilde{\mathbf{M}}_k$. In this letter, this is based on [12]; the kth base channels of spatial details $\mathbf{D}_k^{\mathbf{P}}$ of $\mathbf{P}_k$ are defined as

$$\mathbf{D}_k^{\mathbf{P}} = \mathbf{P}_k - \mathbf{P}_k^{\mathrm{LP}} \tag{4}$$

where $\mathbf{P}_k$ indicate the histogram-matched $\mathbf{P}$ with respect to $\widetilde{\mathbf{M}}_k$, and $\mathbf{P}_k^{\mathrm{LP}}$ is produced by the kth Gaussian low-pass filter whose transfer function matches the shape of MTF of the MS sensor. In more detail, $\mathbf{P}_k^{\mathrm{LP}} = [(\mathrm{MTF}^{\widetilde{\mathbf{M}}_k} \otimes \mathbf{P}_k) \downarrow r] \uparrow r$, where $\otimes$ denotes the convolution operator, $\downarrow r$ refers to a decimation operator which uses *nearest* interpolation by a factor of r (ratio of spatial resolution), and $\uparrow r$ is an upsampling operation which uses *bicubic* interpolation. Similarly, spatial details $\mathbf{D}_k^{\widetilde{\mathbf{M}}}$ of $\widetilde{\mathbf{M}}_k$ are defined as

$$\mathbf{D}_k^{\widetilde{\mathbf{M}}} = \widetilde{\mathbf{M}}_k - \widetilde{\mathbf{M}}_k^{\mathrm{LP}} \tag{5}$$

where $\widetilde{\mathbf{M}}_k^{\mathrm{LP}} = [(\mathrm{MTF}^{\widetilde{\mathbf{M}}_k} \otimes \widetilde{\mathbf{M}}_k) \downarrow r] \uparrow r$.

The missing spatial details of $\widetilde{\mathbf{M}}_k$ may be inferred from the interrelation between $\mathbf{P}_k$ and $\widetilde{\mathbf{M}}_k$. In other words, the issue to be addressed is how to model the relationship between the spatial details of $\mathbf{P}_k$ and $\widetilde{\mathbf{M}}_k$. Normally, the spatial details of $\mathbf{P}_k$ contain details that should not be injected locally or globally into $\widetilde{\mathbf{M}}_k$. To remove these redundant spatial details, this letter applies the SPCA method. The hypothesis behind the proposed fusion method is that the redundant spatial details are concentrated in the PC-1 which is statistically *partially orthogonal* to the unknown spatial details of the high-resolution MS images. This assumption is reasonable because spectrally nonoverlapping MS and PAN bands share not only less radiometric information, but also geometric information in terms of local and global scales. This would inevitably lead to a statistically *partial orthogonality* between PC-1 of $\mathbf{D}_k^{\mathbf{P}}$ and spatial details of unavailable high-resolution MS images. To sum up, the proposed image fusion method can be explained as follows.

1) $\mathbf{D}_k^{\mathbf{P}}$ in (4) is divided into overlapping n by n patches. Border pixels of $\mathbf{D}_k^{\mathbf{P}}$ were padded with mirror reflection to make the final spatial details to the same size as that of $\mathbf{D}_k^{\mathbf{P}}$.
2) All the overlapping patches are transformed into vectors via *lexicographic* ordering. Following the split along the overlapping patches, the *rows* and *columns* of the patch-partitioned $\mathbf{D}_k^{\mathbf{P}}$ are matched in size to that of the original *rows* and *columns* in addition to attaining n^2 *bands*.
3) The PCA (referred to as the SPCA) is applied to the patch-partitioned $\mathbf{D}_k^{\mathbf{P}}$ array. As a result, the PC-1 contains the most variant spatial details from $\mathbf{D}_k^{\mathbf{P}}$, while the rest of information of the $\mathbf{D}_k^{\mathbf{P}}$ array is mapped into the other component (PC-2 to PC-end). Specifically, PC-1 denotes the spatial details shared by all the patch-partitioned $\mathbf{D}_k^{\mathbf{P}}$, while the spatial details specific to each patch-partitioned $\mathbf{D}_k^{\mathbf{P}}$ is accounted by the PC-2 to PC-end components.
4) The PC-1 is replaced by $\mathbf{D}_k^{\widetilde{\mathbf{M}}}$, which is histogram matched to PC-1, followed by the application of inverse PCA. Finally, the *lexicographic column* vectors are mapped to each corresponding overlapping patches to produce new spatial details $\mathbf{D}_k^{\mathbf{N}}$ without local and global redundancies. In other words, the round $(n^2/2)th$ image of $\mathbf{D}_k^{\mathbf{N}}$ contains newly rearranged spatial details based on $\mathbf{D}_k^{\widetilde{\mathbf{M}}}$ as PC-1. This is the key idea behind the proposed fusion method.
5) The final fused MS images $\hat{\mathbf{M}}_k$ are given by following expression:

$$\hat{\mathbf{M}}_k = \widetilde{\mathbf{M}}_k + \Gamma \circ \mathbf{D}_k^{\mathbf{N}}. \tag{6}$$

In summary, the spatial details can be inferred and transferred effectively through the local and global injection gains given in (3) to resolve the over- and under-sharpening problems. Also, the proposed fusion method can construct the effective and necessary spatial details by replacing PC-1 of $\mathbf{D}_k^{\mathbf{P}}$ with $\mathbf{D}_k^{\widetilde{\mathbf{M}}}$ which results in eliminating the spatial redundancies of the PAN image, thereby rearranging $\mathbf{D}_k^{\mathbf{P}}$ with reference to $\mathbf{D}_k^{\widetilde{\mathbf{M}}}$. Considering this approach, the proposed fusion method can be regarded as a hybrid method integrating both CS and MRA-based fusion methods.

IV. Experiments and Discussion

Experiments were conducted to evaluate the performance of the proposed method using two WorldView-2 data sets. The WorldView-2 satellite provides a PAN band and eight MS bands. Among these MS bands, the band-1 (Coastal) and band-8 (Near-IR2) do not spectrally overlap with respect to the PAN band, while band-7 (Near-IR1) partially coincides. The size of the MS image was 512×512 pixels, and that of the PAN image was 2048×2048 pixels. The proposed method was compared with the ARSIS method [15], guided filter [5], bilateral filter [6], nonlinear intensity-hue-saturation (NIHS) method [16], SR-based method [4], and partial replacement adaptive CS (PRACS) method [17]. The parameters of each method are manually tuned to achieve the best performance. The evaluation of the fusion methods focused on the *synthesis* property [18], as the spatial resolutions of the MS and PAN images were first degraded, then fused, and compared with the original MS imagery. The MTF-based filtering and decimation were applied to degrade the resolution. The Nyquist frequencies of the MS bands were 0.35 for band-1 to band-7, 0.27 for band-8, and 0.11 with regard to the PAN band. Also, the moving window size for SPCA was determined experimentally at 7×7, yet returned the best results in this letter (see Tables I and II).

A. Visual Analysis

The study area of the first data set is San Francisco, CA, USA, and the visual performances of the fused images are shown in Fig. 2. The ARSIS method demonstrated slightly bluish results, while NIHS and PRACS methods returned results of lower sharpness. The guided filter-based method was determined to have less injection of local spatial details in comparison to the bilateral filter-based method. On the other hand, the proposed fusion method produced local spatial

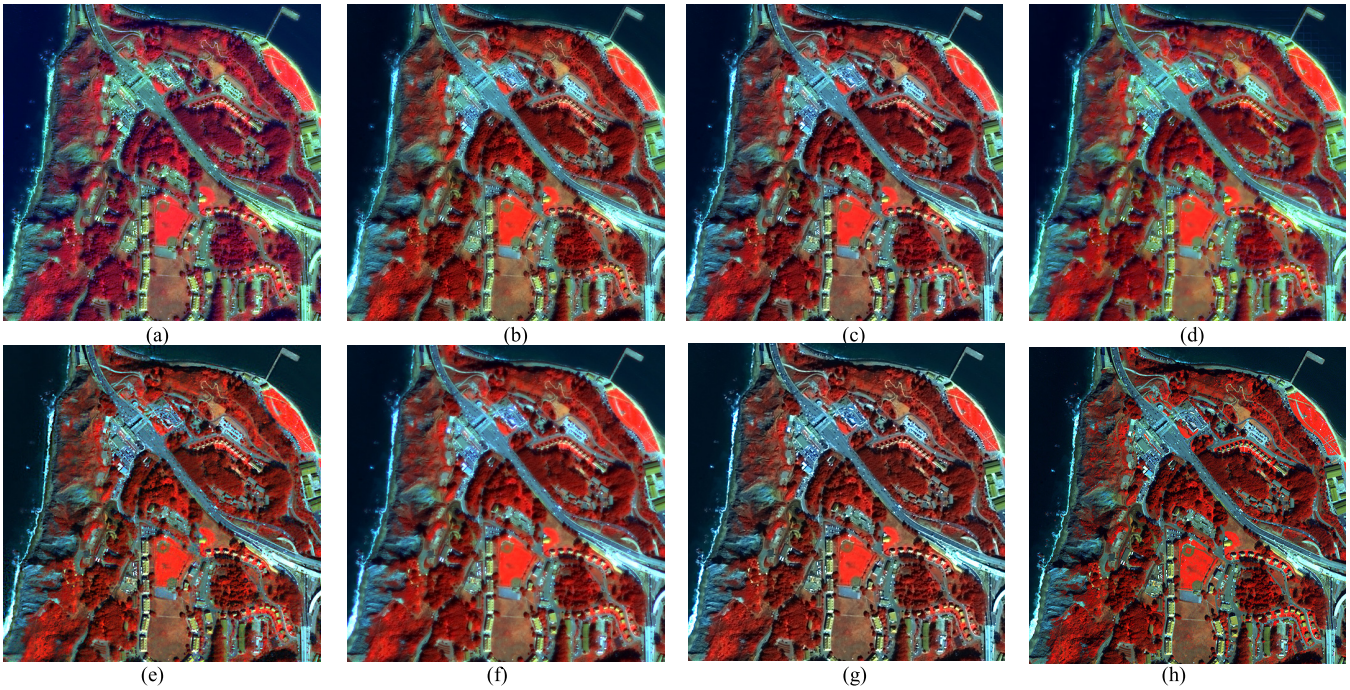

Fig. 2. Fused images of the San Francisco data set obtained by different methods (MS-8, 4, and 1 bands to RGB combination). (a) ARSIS method [15]. (b) Guided filter [5]. (c) Bilateral filter [6]. (d) NIHS method [16]. (e) SR-based method [4]. (f) PRACS method [17]. (g) Proposed method. (h) Reference MS imagery.

TABLE I
EVALUATION OF THE SAN FRANCISCO DATA SET

Fusion Methods		SAM (0)	Corr (1)	ERGAS (0)	Q-index (1)
ARSIS method [15]		6.5904	0.9231	5.2583	0.7280
Guided filter [5]		5.9923	0.9245	5.3277	0.7240
Bilateral filter [6]		5.8127	0.9343	4.8929	0.7607
NIHS method [16]		6.5463	0.9199	5.8449	0.6755
SR-based method [4]		6.7475	0.9343	5.0058	0.7384
PRACS method [17]		6.2101	0.9235	5.3540	0.7184
Proposed method	3×3	6.4216	0.8950	5.7593	0.6977
	5×5	6.2255	0.9206	5.0876	0.7488
	7×7	5.6926	0.9454	4.4847	0.7934
	9×9	5.7024	0.9454	4.4978	0.7928

TABLE II
EVALUATION OF THE WASHINGTON, DC, USA, DATA SET

Fusion Methods		SAM (0)	Corr (1)	ERGAS (0)	Q-index (1)
ARSIS method [15]		6.7287	0.9383	4.6596	0.7930
Guided filter [5]		6.7135	0.9352	4.8746	0.7644
Bilateral filter [6]		6.3976	0.9462	4.2949	0.8103
NIHS method [16]		6.6610	0.9349	5.0695	0.7433
SR-based method [4]		7.5956	0.9421	4.3051	0.8001
PRACS method [17]		6.6693	0.9347	4.7697	0.7577
Proposed method	3×3	6.5506	0.9056	5.5218	0.7298
	5×5	6.4505	0.9291	4.8146	0.7849
	7×7	6.2524	0.9572	3.7092	0.8447
	9×9	6.4857	0.9359	4.6981	0.8073

details that were visually better than the SR-based method and ultimately showed results that were the most similar to the reference MS imagery. The second study area is Washington, DC, USA, and the fused images are shown in Fig. 3. Similar to the first study area, the proposed fusion method demonstrated the most similar results with respect to the reference MS images for the second study area. In particular, buildings and vegetation areas were shown to have a relatively higher sharpness in comparison to the other fusion methods. In these two cases, as shown in Figs. 2 and 3, we concluded that the proposed method can, therefore, provide visually satisfactory results with regard to the reference MS images.

B. Quantitative Assessment

Multiple measures of image quality have been employed to evaluate the quality of the fused images. The spectral angle mapper, Corr, the relative dimensionless global error in synthesis (ERGAS), and Q-index were used as measures of radiometric and geometric distortions in this letter. Ideal values of each quality index are represented in parentheses. In-depth discussion of quality assessment protocols can be found in the recent work [18]. Tables I and II demonstrate that the experimental results and the proposed fusion method produced the most optimal quantitative results for each category. At the bottom of Tables I and II, $n \times n$ represents the size of overlapping patches of the proposed method. The bilateral filter-based method was determined to have the second best results. Most importantly, the proposed method returned the lowest value in the root-mean-square error-based ERGAS measure, as well as the highest value in the Q-index, displaying an effectiveness of the proposed method in fusing spectrally nonoverlapping MS imagery like WorldView-2. Such spectrally mismatching problems or band assignment for image fusion is also an important issue when fusing the MS and HS imageries. Further studies using the MS and HS data will, therefore, be addressed in our future works to apply the proposed fusion method.

Fig. 3. Fused images of the Washington, DC, USA, data set obtained by different methods (MS-5, 3, and 2 bands to RGB combination). (a) ARSIS method [15]. (b) Guided filter [5]. (c) Bilateral filter [6]. (d) NIHS method [16]. (e) SR-based method [4]. (f) PRACS method [17]. (g) Proposed method. (h) Reference MS imagery.

V. Conclusion

In this letter, a local and global injection model using the MS, PAN, and low-resolution PAN images was proposed, which decisively influences the quality of the fused imagery. Furthermore, to make the necessary spatial details, as well as to remove the redundancies in spatial details of the PAN image, new spatial details were constructed by applying the SPCA method and MTF-based filters. In the fusion process, new injection gains and the proposed spatial details were combined to generate high-quality MS imagery in terms of spatial and spectral information, and experiments using WorldView-2 data sets were conducted to achieve satisfying results. In light of this improvement, we hope that these results will help to propel research with various high-resolution MS images on remote sensing applications in the future.

Acknowledgment

The authors would like to thank X. Lu [15], J. Liu [5], N. H. Kaplan [6], and R. Restaino [4] for providing their MATLAB codes. They would also like to thank the editors and two anonymous reviewers for their valuable comments and suggestions which have greatly helped improve this letter.

References

[1] Y. Zhang, "Understanding image fusion," *Photogramm. Eng. Remote Sens.*, vol. 70, no. 6, pp. 653–660, Jun. 2004.
[2] G. Vivone *et al.*, "A critical comparison among pansharpening algorithms," *IEEE Trans. Geosci. Remote Sens.*, vol. 53, no. 5, pp. 2565–2585, May 2015.
[3] L. Loncan *et al.*, "Hyperspectral pansharpening: A review," *IEEE Trans. Geosci. Remote Sens.*, vol. 3, no. 3, pp. 27–46, Sep. 2015.
[4] M. R. Vicinanza, R. Restaino, G. Vivone, M. Dalla Mura, and J. Chanussot, "A pansharpening method based on the sparse representation of injected details," *IEEE Geosci. Remote Sens. Lett.*, vol. 12, no. 1, pp. 180–184, Jan. 2015.
[5] J. Liu and S. Liang, "Pan-sharpening using a guided filter," *Int. J. Remote Sens.*, vol. 37, no. 8, pp. 1777–1800, Apr. 2016.
[6] N. H. Kaplan and I. Erer, "Bilateral filtering-based enhanced pansharpening of multispectral satellite images," *IEEE Geosci. Remote Sens. Lett.*, vol. 11, no. 11, pp. 1941–1945, Nov. 2014.
[7] Y. Kim, Y. Eo, Y. Kim, and Y. Kim, "Generalized IHS-based satellite imagery fusion using spectral response functions," *ETRI J.*, vol. 33, no. 4, pp. 497–505, Aug. 2011.
[8] Q. Wang, P. Yan, Y. Yuan, and X. Li, "Multi-spectral saliency detection," *Pattern Recognit. Lett.*, vol. 34, no. 1, pp. 34–41, 2013.
[9] F. D. van der Meer *et al.*, "Multi- and hyperspectral geologic remote sensing: A review," *Int. J. Appl. Earth Observ. Geoinf.*, vol. 14, no. 1, pp. 112–128, Feb. 2012.
[10] C. Thomas, T. Ranchin, L. Wald, and J. Chanussot, "Synthesis of multispectral images to high spatial resolution: A critical review of fusion methods based on remote sensing physics," *IEEE Trans. Geosci. Remote Sens.*, vol. 46, no. 5, pp. 1301–1312, May 2008.
[11] H. R. Shahdoosti and H. Ghassemian, "Combining the spectral PCA and spatial PCA fusion methods by an optimal filter," *Inf. Fusion*, vol. 27, pp. 150–160, Jan. 2016.
[12] B. Aiazzi, L. Alparone, S. Baronti, A. Garzelli, and M. Selva, "MTF-tailored multiscale fusion of high-resolution MS and pan imagery," *Photogramm. Eng. Remote Sens.*, vol. 72, no. 5, pp. 591–596, May 2006.
[13] S. Rahmani, M. Strait, D. Merkurjev, M. Moeller, and T. Wittman, "An adaptive IHS pan-sharpening method," *IEEE Geosci. Remote Sens. Lett.*, vol. 7, no. 4, pp. 746–750, Oct. 2010.
[14] Y. Leung, J. Liu, and J. Zhang, "An improved adaptive intensity–hue–saturation method for the fusion of remote sensing images," *IEEE Geosci. Remote Sens. Lett.*, vol. 11, no. 5, pp. 985–989, May 2014.
[15] X. Lu, J. Zhang, T. Li, and Y. Zhang, "Pan-sharpening by multilevel interband structure modeling," *IEEE Geosci. Remote Sens. Lett.*, vol. 13, no. 7, pp. 892–896, Jul. 2016.
[16] M. Ghahremani and H. Ghassemian, "Nonlinear IHS: A promising method for pan-sharpening," *IEEE Geosci. Remote Sens. Lett.*, vol. 13, no. 11, pp. 1606–1610, Nov. 2016.
[17] J. Choi, K. Yu, and Y. Kim, "A new adaptive component-substitution-based satellite image fusion by using partial replacement," *IEEE Trans. Geosci. Remote Sens.*, vol. 49, no. 1, pp. 295–309, Jan. 2011.
[18] F. Palsson, J. R. Sveinsson, M. O. Ulfarsson, and J. A. Benediktsson, "Quantitative quality evaluation of pansharpened imagery: Consistency versus synthesis," *IEEE Trans. Geosci. Remote Sens.*, vol. 54, no. 3, pp. 1247–1259, Mar. 2016.